

## HYDROGEOLOGICAL SPRING CHARACTERIZATION IN THE VAJONT AREA

PAOLO FABBRI<sup>(\*)(\*\*)</sup>, MIRTA ORTOMBINA<sup>(\*)</sup>, LEONARDO PICCININI<sup>(\*)</sup>,  
DARIO ZAMPIERI<sup>(\*)</sup> & LUCA ZINI<sup>(\*\*\*)</sup>

<sup>(\*)</sup>Università degli Studi di Padova - Dipartimento di Geoscienze - Via G. Gradenigo, 6 - Padova, Italy

<sup>(\*\*)</sup>Consiglio Nazionale delle Ricerche (C.N.R.) - Istituto di Geoscienze e Georisorse - Padova, Italy

<sup>(\*\*\*)</sup>Università degli Studi di Trieste - Dipartimento di Matematica e Geoscienze - Via Weiss, 2 - Trieste, Italy

### ABSTRACT

The Vajont Valley is mainly known for the catastrophic event of 9 October 1963, when a vast landslide occurred on the southern slope of the Vajont dam reservoir, causing a giant wave of water that flooded the Piave Valley below. Since then, many studies of the geological and geomechanical aspect of the landslide have been carried out, while very few studies have focused on the hydrogeological characteristics of this area. This paper proposes a hydrogeological conceptual model for the carbonate aquifers of the Vajont area, based on the continuous monitoring of two springs and environmental isotope investigations. Cross-correlation functions between time series and the VESPA index were used to delineate groundwater flow systems and the degree of karstification. This model has been confirmed by analyses of the amounts of stable isotopes, such as <sup>18</sup>O and <sup>3</sup>H, in precipitation and groundwater.

**KEY WORDS:** *Vajont, spring, continuous monitoring, cross-correlation function, VESPA index, environmental isotopes*

### GEOLOGICAL AND HYDROGEOLOGICAL SETTINGS

This paper focuses on the hydrogeological characteristics of the Vajont area. The study site is located in the municipalities of Erto-Casso (Friuli Venezia Giulia region) and Longarone (Veneto region) in the southeastern part of the Dolomite Mountains, northeastern Italy. This area is bounded by Mt. Salta (2,039 m above sea level [a.s.l.]) and Mt. Borgà (2,215 m a.s.l.) on the north, the

Gallina Valley on the south, the Piave River on the west and the Zemola and Mesazzo valleys on the east (Fig. 1).

The landscape of Vajont valley was severely altered by the catastrophe of 9 October 1963, when a vast deposit of the Mt. Toc landslide completely blanketed the bottom of the valley producing an enormous wave of at least 30 million cubic metres of water which flooded the Piave Valley below.

Despite a large body of geological and geomechanical literature mainly concerning the Vajont disaster (MULLER, 1964, 1968, 1987; SEMENZA, 1965; CORBIN, 1982; HENDRON & PATTON, 1985; BELLONI & STEFANI, 1987; NONVEILLER, 1987; GHIROTTI, 1994; TIKA & HUTCHINSON, 1999; SEMENZA & GHIROTTI, 2000; KILBURN & PETLEY, 2003; MANTOVANI & VITAFINZI, 2003; HELMSTETTER *et alii*, 2004; GENEVOIS & GHIROTTI, 2005; VEVEAKIS *et alii*, 2007; WARD & DAY, 2011), hydrogeological investigations are few (BESIO, 1986). This is most likely due to the relatively shallow and poor groundwater circulation before the disaster, currently shown by the absence of springs in the Mt. Toc area and by the very low spring flow rates in the Vajont Valley.

The bedrock of the study area belongs to the eastern South Alpine structural unit, which represents the Neogene-Present back-thrusted (south vergent) part of the Alpine chain. The Vajont Valley coincides with the core of an Alpine syncline (Erto syncline) with an axis trending approximately E-W and gently plunging to the east (RIVA *et alii*, 1990). The exposed deformed rocks are Liassic to Eocene carbonates and marls (SE-

MENZA, 1965); the Upper Triassic Dolomia Principale crops out only in the neighboring valleys. The northern limb of the Erto syncline is reversed and stretched, lying just at the foot of the Mt. Borgà thrust (Mt. Salta thrust in RIVA *et alii*, 1990) with its Spesse thrust play, which consists of two older thrusts passively transported in reverse style by the Belluno thrust.

The Vajont landslide occurred on the Erto syncline's south limb, which dips 30° to 50° to the north-northeast (western sector) and north (eastern sector). The landslide rupture surface is localized within the Middle-Upper Jurassic Fonzaso Formation, a sequence of thinly stratified limestones with thin (0.1-5 cm) intercalations of clays (HENDRON & PATTON, 1985). The sliding layered sequence was laterally constrained by a system of southward-converging subvertical faults (the Croda Bi-

anca and Col Tramontin faults on the east and the west branch of the Col delle Erghene fault on the west), while the landslide crown was constrained by E-W-trending structures (Col delle Erghene fault; RIVA *et alii*, 1990).

The succession of strata and their relative permeabilities are shown in Tab. 1.

From a hydrogeological point of view, only the Zemola Valley contains several significant springs, whereas the area around Mt. Toc is characterized by less surface water and fewer springs, most of which display low levels of discharge. This situation, we believe, is due to karstic groundwater circulation. This hypothesis is based on direct observation of sinkholes on the upper slope of the Vajont landslide; in this area, the majority of meteoric waters infiltrate without leading to a significant surface flow. The presence of karst phenomena in this

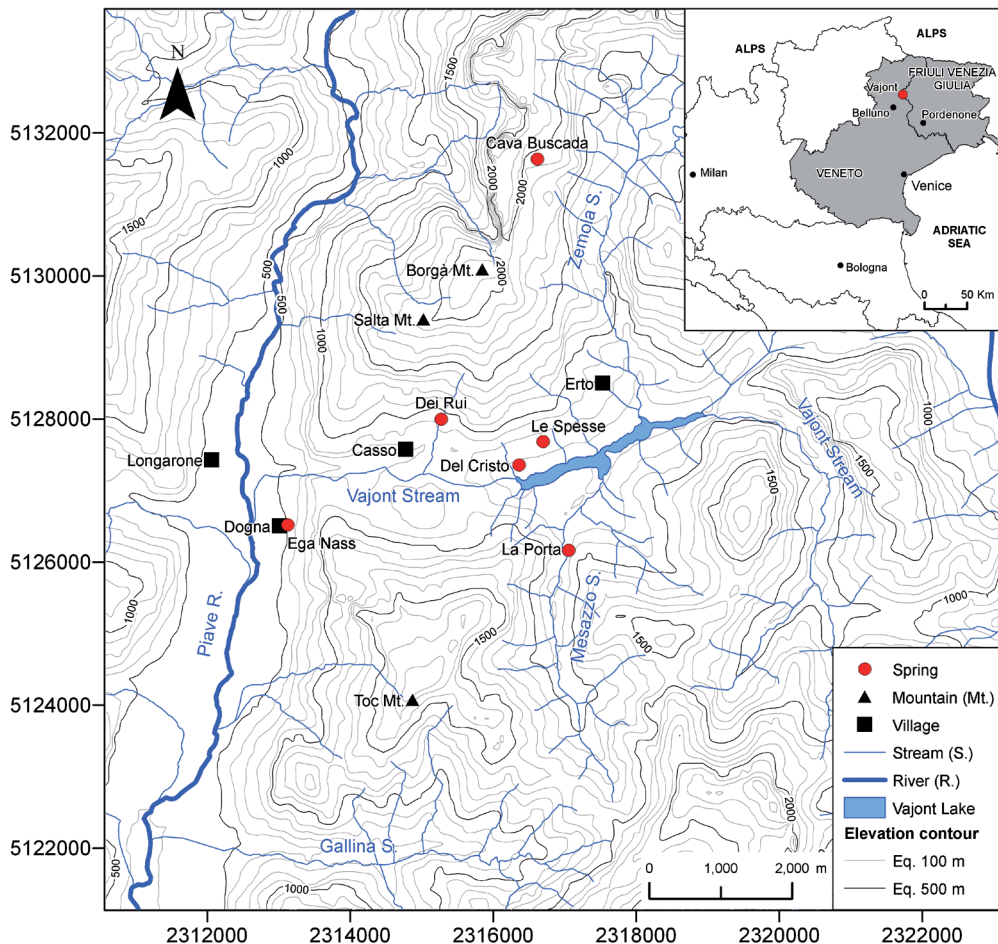


Fig. 1 - Geographic setting of the Vajont area (coordinates and elevations are in meters, datum Roma 1940, Gauss Boaga - Est)

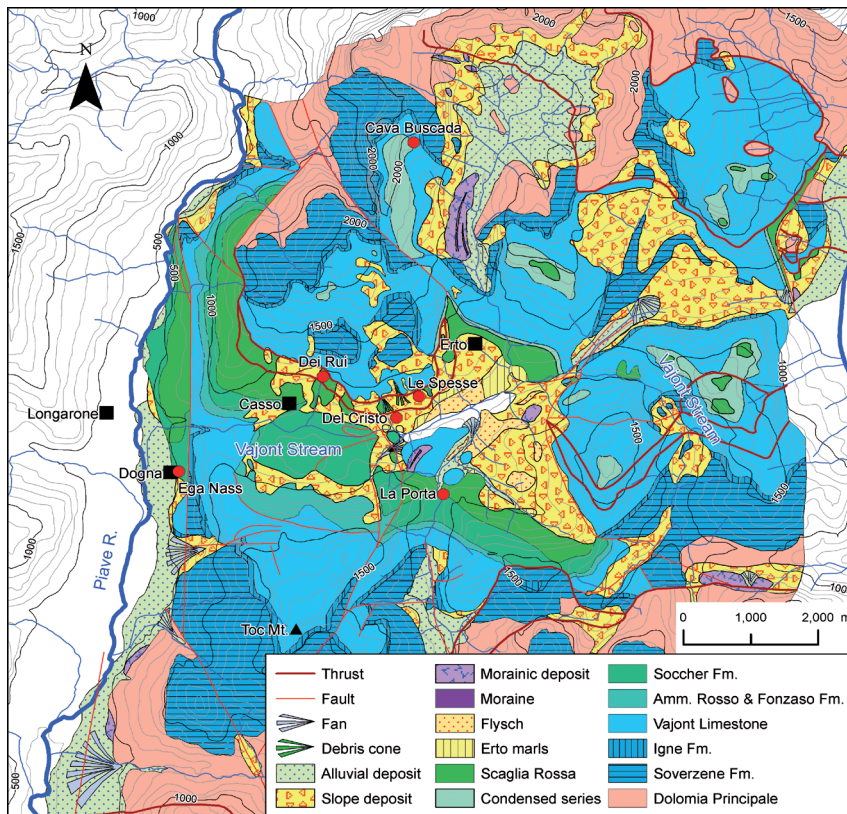


Fig. 2 - Geological sketch map of the study area (partly from RIVA et alii, 1990); red dots are the monitoring springs

Tab. 1 - Main lithologic units of the Vajont area and their relative permeability (units symbols correspond to label in the Fig. 7)

Unit	Age	Permeability
Quaternary deposits -alluvial deposits ( <i>Dal</i> ) -slope deposits ( <i>Dvers</i> ) -glacial deposits ( <i>Dmor</i> )	Quaternary	Very high
Flysch ( <i>F</i> )	Eocene	Very low
Erto marls ( <i>Me</i> )	Paleocene	Very low
Scaglia Rossa ( <i>Sr</i> )	Upper Cretaceous–Lower Paleocene	Low (B)
Condensed series ( <i>Sc</i> )	Malm–Upper Cretaceous	Very low
Soccher Formation ( <i>Fsh</i> )	Lower–Upper Cretaceous	Medium
Fonzaso Fm. ( <i>ArFf</i> ) and Ammonitico Rosso	Malm–Lower Cretaceous	Very low
Vajont Limestones ( <i>Cv</i> )	Dogger	High
Igne Formation ( <i>I</i> )	Upper Lias	Very low
Soverzene Formation ( <i>Fs</i> )	Middle and Lower Lias	Medium
Dolomia principale ( <i>Dp</i> )	Upper Triassic.	Medium

area is well reported in the geologic literature (HENDRON & PATTON, 1985; SEMENZA & GHIROTTI, 2000).

In the study area, twenty springs were identified. Most of them have very low discharge (< 1 L/s) and similar physico-chemical parameters. Chemical analyses were carried out on water from eight springs (sodium, calcium, potassium, magnesium, total hardness, total dissolved solids [TDS], iron, manganese, methyl orange alkalinity, chloride, sulphate, carbonate), and they could be classified as oligomineral (135 < TDS <

210 mg/l), cold (6.7 < T < 10°C) and calcium magnesium bicarbonate-type waters; furthermore, all the springs have a slightly alkaline pH ranging between 8 and 8.4, Eh ranging from 182 to 274 mV and electrical conductivity ranging from 162 to 281 µS/cm. These physico-chemical data suggest the presence of young waters with short travel paths. The locations of five of these springs are shown in Fig. 2, and their corresponding Schoeller diagrams are plotted in Fig. 3.

After a reconnaissance of the geology of the study

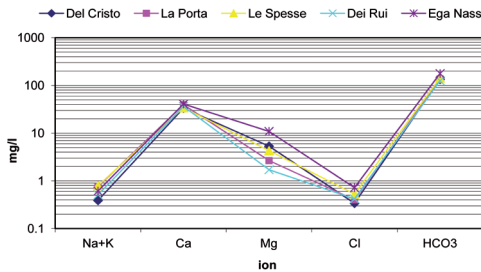


Fig. 3 - Schoeller diagrams of five springs

area, two springs with appropriate features were chosen for continuous monitoring; Ega Nass spring, on the west side of Mt. Toc (Dogna, Longarone), and Le Spesse spring, on the opposite side of the Vajont landslide (Le Spesse, Erto-Casso). In July and September 2010, two data-loggers (Diver) were installed to measure the hourly discharge, electrical conductivity (EC) and temperature (T) of the spring waters. These data were compared with rainfall from two weather stations (ARPAV and Servizio Idrografico Regione Friuli Venezia Giulia) to identify correlations between spring behavior (discharge, temperature and electrical conductivity) and rainfall events.

## HYDROGEOLOGICAL BEHAVIOR OF LE SPESSE AND EGA NASS SPRINGS

### LE SPESSE SPRING

Le Spesse spring (Figs. 2 and 4) is situated at an elevation of approximately 810 m a.s.l. close to a small hamlet in the municipality of Erto Casso (Pordenone). This spring is located west of Erto Casso, on the north side of the Vajont Valley and east of the Vajont dam, at the foot of the southern slope of Mt. Borgà. The spring emerges from the Quaternary deposits; however, after evaluating the cross section (Fig. 7), in particular the formations next to the spring, it is evident that this spring water originates in the Vajont Limestone (high permeability), which is tectonically juxtaposed against the Scaglia Rossa Formation (low permeability), and flows through and emerges from the Quaternary deposits (Fig. 6a). According to the hydrogeological classification proposed by CIVITA (1972), which takes into account the point of emergence, this spring can be classified as a spring of contact between units of highly contrasting permeability.

### EGA NASS SPRING

Ega Nass spring (Fig. 5) is located on the west

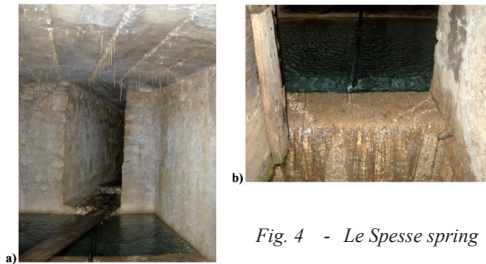


Fig. 4 - Le Spesse spring



Fig. 5 - Ega Nass spring

slope of Mt. Toc, on the east side of the Piave Valley, at an elevation of 515 m a.s.l., at Dogna (municipality of Longarone). The Vajont Limestone (high permeability) underlies the Ega Nass spring recharge area. The Vajont Limestone overlies the Igne Formation (very low permeability). The spring emerges at the exposed contact between these two units. The Vajont Limestone is characterized by a high degree of karstification. The location of this spring may also be controlled by a system of faults parallel and orthogonal to the slope (Figs. 6b and 7).

The measured discharge of the Ega Nass spring does not represent the total flow emerging because spring water emerges from several points beyond our monitoring station at the main discharge location.

## DATA MONITORING ANALYSIS

### LE SPESSE

An analysis of Figure 8 shows a relationship between the rainfall (P) and the spring flow rate (Q). Moreover a cross-correlation investigation has helped us to quantify the lag times over short time periods. Lagged correlation refers to the correlation between two time series at different lags, or offsets in time. The cross-correlation function (CCF) is the correlation, related to the two time series, as a function of lag. The sample cross

Fig. 6 - Hydrogeological sketch map of the Le Spesse (a) and Ega Nass (b) springs. The elevations of the topographic contour lines are in meters

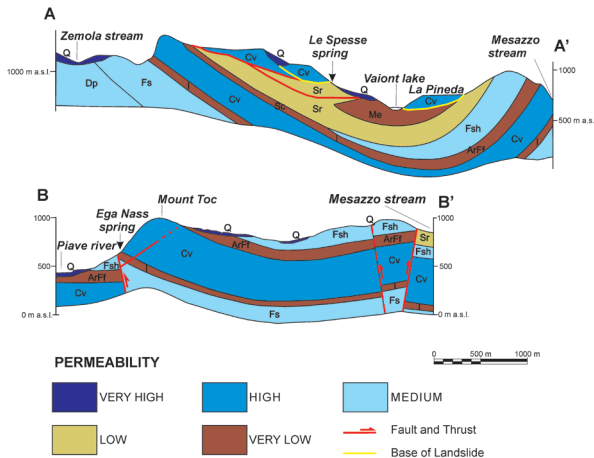
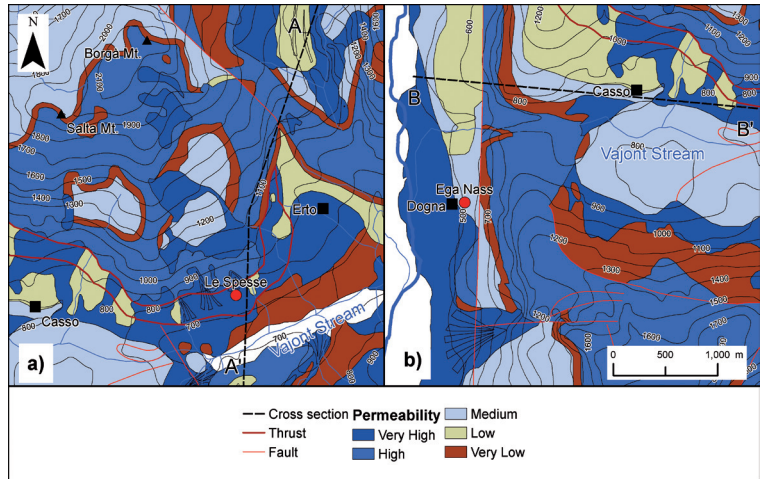


Fig. 7 - Hydrogeological cross sections through Le Spesse and Ega Nass springs. Cross section line locations are shown in Figures 6a and 6b, respectively. Symbols representing geologic units are explained in Table 1

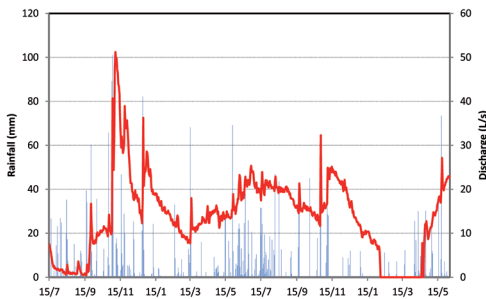


Fig. 8 - Comparison between daily rainfall (light blue histogram) and Le Spesse flow rate (red line) from 15 July 2010 to 4 June 2012

covariance function is given by the following equation:

$$c_{uy} = \frac{1}{N} \sum_{t=1}^{N-k} (u_t - \bar{u})(y_{t+k} - \bar{y}) \quad [k = 0, 1, 2, \dots, (N-1)]$$

$$c_{uy} = \frac{1}{N} \sum_{t=1-k}^N (u_t - \bar{u})(y_{t+k} - \bar{y}) \quad [k = -1, -2, \dots, -(N-1)]$$

where N is the series length,  $\bar{u}$  and  $\bar{y}$  are the sample means and k is the lag. The sample cross-correlation is the cross-covariance of the two series divided by their standard deviations:

$$r_{uy}(k) = \frac{c_{uy}(k)}{\sqrt{c_{uu}(0)c_{yy}(0)}}$$

The cross-correlation function (CCF; P vs Q) in Figure 9 shows a significantly positive correlation at lag 1, which means that the most important response in flow rate (output) occurs beginning 1 day after a rainfall event (input). Moreover, a less evident positive cross-correlation at lag 0 also indicates a certain temporal association between rainfall and the spring flow rate.

In a situation of a quick flow-rate response to rainfall events, it can be useful to compare spring water temperature ( $T_s$ ) with atmospheric temperature ( $T_a$ ) to ascertain whether the flow-rate increase is due to a “piston” effect or to a local rainfall infiltration.

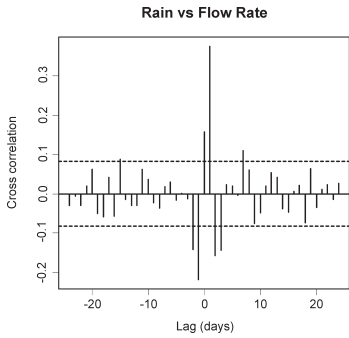


Fig. 9 - Cross-correlation of rainfall and spring flow rates

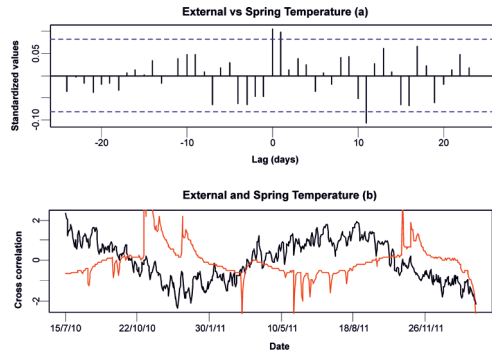


Fig. 10 - (a) Cross-correlation between  $T_a$  and  $T_s$ ; (b) comparison between atmospheric temperature (black line) and water spring temperature (red line)

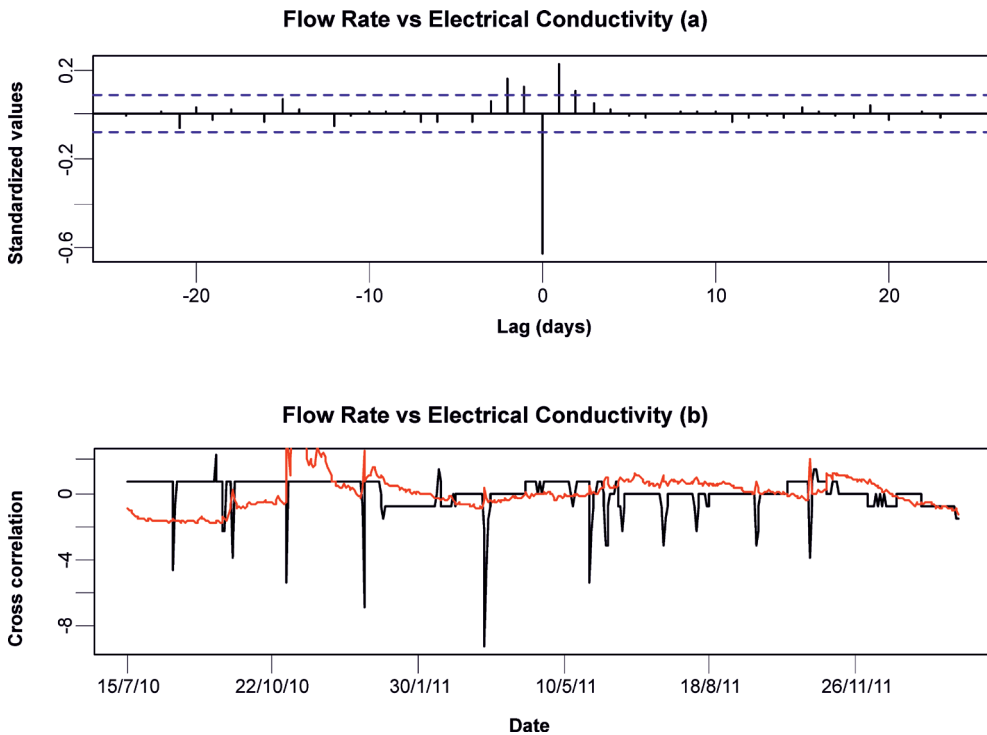


Fig. 11 - (a) Cross-correlation between spring flow rate and electrical conductivity; (b) comparison between spring flow rate (red line) and electrical conductivity (black line)

Analysis of Figure 10a shows a positive cross-correlation between variations in  $T_a$  and variations in  $T_s$  at lag 0 and lag 1, indicating that the water temperature variations in the short term are strictly linked to the atmospheric temperature variations. Moreover the temperature trend comparison in Figure 10b shows a reverse trend: in winter the  $T_a$  is lower and the  $T_s$  is higher, while the reverse was observed in summer. During the warm season, the temperature of spring

water is colder than that in the cold season, meaning that the water discharge is in partial equilibrium with the reservoir temperature instead of with the atmospheric temperature. Evidently, the travel time through the aquifer is insufficient for water to reach a thermal equilibrium with the rock matrix: in the winter, warm water discharges represent infiltration from the previous summer, and in the summer, outflowing cold water represents infiltration from the previous winter. Only

Fig. 12 - (a) Cross-correlation between rainfall ( $P$ ) vs electrical conductivity ( $EC$ ); (b) comparison between rainfall (red histogram) and electrical conductivity (black line)

during rainy days (short time periods) are  $T_s$  variations influenced by variations in atmospheric temperatures, due to the effects of local rainfall infiltration, as seen in the cross-correlations in Figure 10a.

A comparison between the spring flow rate ( $Q$ ) and electrical conductivity ( $EC$ ; Fig. 11) shows a negative cross correlation at lag 0 (e.g., when  $Q$  increases then the  $EC$  decreases and vice versa). Thus the relationship shown in Figure 11 confirms the effect of local rainfall infiltration, which temporarily decreases the  $EC$  of the spring water.

This hypothesis is also confirmed by a negative cross-correlation at lag 1 between rainfall ( $P$ ) and  $EC$  (Fig. 12). In fact the  $EC$  decrease in the spring water at lag 1 corresponds to a maximum positive cross-correlation between flow rate and rainfall, i.e., the dilution of spring water is due to the local rainfall infiltration.

The variations in CCF found in the analyses suggest that local short-term rainfall increase spring flow rates. Other analytical results also show some characteristics of a deeper spring water components, coming from the corresponding aquifer reservoir. Figure 11a shows a visible positive cross-correlation between  $Q$  and  $EC$  at lag 1, i.e., an increase in  $Q$  produces an increase in  $EC$ . This trend can be explained as more-conductive coming from the reservoir; this signal is not as pronounced as that from lag 0 (superficial infiltration) but is nevertheless statistically significant. In addition, a positive cross-correlation was seen between  $Q$  and  $T_s$  at lag 0 (Fig. 13a); i.e., an increase in  $Q$  is positively correlated with an increase in  $T_s$ . Figure 13b shows an at lag 0 and 1 (Fig. 15a). However, Figure 15b shows a similar temperature trend in winter, while in sum-

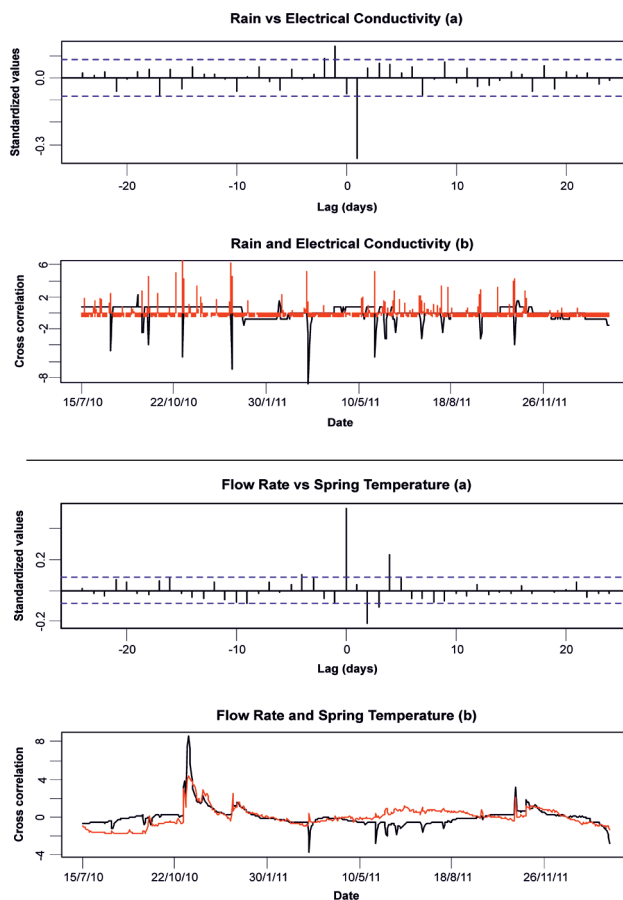


Fig. 13 - (a) Cross-correlation of spring flow rate ( $Q$ ) vs spring water temperature ( $T_s$ ); (b) comparison between water temperature (black line) and flow rate of the spring (red line)

increase in  $T_s$  in winter that is positively correlated to an increase in  $Q$ , while in summer the reverse is seen. This reversal is most likely because, during the dry season, the low flow rate allows a partial equilibrium with the rock matrix.

### EGANASS

Analysis of the data from EgaNass spring tends to be less informative (than that from Le Spesse spring) because of problems related to functioning of the data-logger during the monitoring period.

Analysis of Figure 14a seems to indicate a relationship between  $P$  and  $Q$ , but CCF analysis yields no significant cross-correlations (Fig. 14b).

Analyses of atmospheric and spring water temperatures confirm a local influence of shallow infiltrating waters associated with a positive cross-correlation

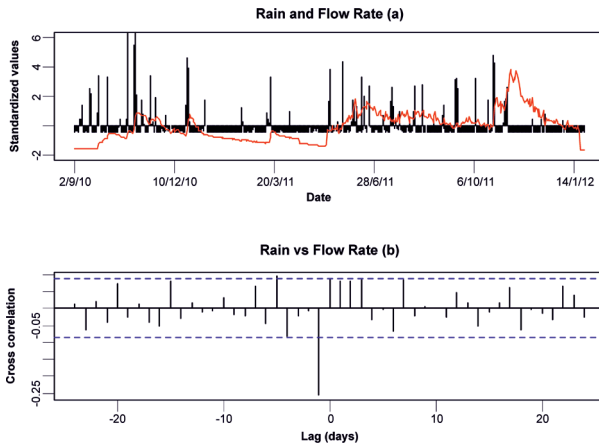


Fig. 14 - (a) Rainfall (black histogram bars) plotted against spring flow rate (red line); (b) CCF between rainfall and spring flow rates

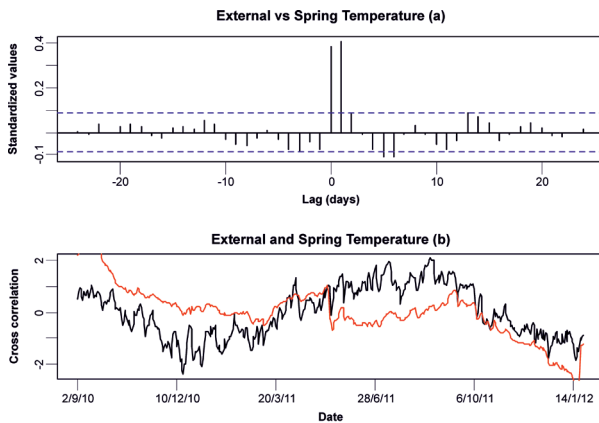


Fig. 15 - (a) CCF between atmospheric temperature ( $T_a$ ) and spring water temperature ( $T_s$ ); (b) comparison between atmospheric and spring water temperature

mer a partial inversion is seen, as in the corresponding diagram from Le Spesse spring.

Analyses of EC and Q from Le Spesse spring shows a negative cross-correlation but at lags 1 and 2 instead of at lag 0 (Fig. 16a), which means that an increase of Q is associated with a decrease in EC, indicating a superficial component of dilution with a greater lag time. Regrettably, the monitoring period was shorter than that of Le Spesse spring, and the relationship observed might only be an apparent or spurious one.

Problems that are related to the changing of instruments during the monitoring period do not allow a more detailed comparison.

In Figure 16b, where a negative cross-correlation

at lag 1 means that an increase of Q causes a decrease of  $T_s$  and vice versa, the increase in Q is essentially due to rainfall infiltration after one day, after which the decrease in Q is associated with water from the reservoir and an increase in  $T_s$ .

### VESPA INDEX

Because we collected monitoring data spanning more than one year, the VESPA (Vulnerability Estimator for Spring Protection Areas) index was calculated to quantify the vulnerability of Le Spesse spring. This index is an estimate of vulnerability based on an analysis of spring hydrographs. The VESPA index (GALLEANI *et alii*, 2011) takes into account the discharge (Q), water spring temperature (T) and electrical conductivity (EC), based on 1 year of monitoring data from spring discharge.

It is well known that different hydrographs represent different aquifers (AMIT *et alii*, 2002; MALVICINI *et alii*, 2005). Every aquifer drainage system has an impulse function transforming an input, for example rainfall, into output parameters such as discharge, temperature and EC variations. Such an analysis may provide information regarding groundwater network connectivity (PLAGNES & BAKALOWICZ, 2001; VIGNA, 2007; KRASIC & STEVANOVIC, 2009).

The equation for calculating the VESPA index is as follows:

$$V = c(\rho) \beta \gamma$$

where  $c(\rho)$  is the correlation factor, represented by  $c(\rho) = [u(-\rho) + 0.5u(\rho)] |\rho|$ ,  $\rho$  is the correlation coefficient between Q and EC related to a time interval of one year and  $u(\rho)$  is the Heavside step function:

$$u(\rho) = \begin{cases} 1, & \rho \geq 0 \\ 0, & \rho < 0 \end{cases}$$

The factor  $\beta$ , the temperature variability factor, is defined as follows:

$$\beta = \left( \frac{T_{max} - T_{min}}{1^\circ C} \right)^2$$

where  $T_{max}$  and  $T_{min}$  are the maximum and minimum temperature, respectively, during the monitored year.

The factor  $\gamma$ , the discharge variability factor, is

defined as follows:

$$\gamma = \frac{Q_{max} - Q_{min}}{Q_m}$$

where  $Q_{max}$ ,  $Q_{min}$  and  $Q_m$  are the maximum, minimum and average discharges, respectively, during the monitored year.

Based on the correlation coefficient, GALLEANI *et alii* (2011) proposed three broad behavioral categories (Tab. 2) representing various levels of network effectiveness and, consequently, various styles of response to an infiltration input.

A Type A spring is one associated with a highly effective drainage system, with well-developed karst conduits, quick, strong discharge, and discharge that is rapidly depleted. This type of system has also been called a hypersensitive karst (HOBBS & SMART, 1986). The value of the annual discharge variability index (MEINZER, 1923) is quite high, with values upwards of 100%.

A Type B spring is associated with a moderately effective drainage system. In these types of aquifers, a certain storage volume is present, and the infiltration produces a typical “piston effect” for mobilizing the resident groundwaters. Groundwater is in thermal equilibrium with its reservoir, and its EC is primarily than that of freshly infiltrated waters. The piston effect produces an increase in Q, EC and T.

A Type C spring is associated with a relatively ineffective drainage system, and the piston effect is barely visible or absent. The discharge displays low fluctuations, with delays of up to several months associated with significant changes in rainfall. The electrical conductivity and temperature show similar trends, with low variations. A large saturated zone is present, and water infiltrations reach equilibrium with the aquifer and resident groundwater; external output due to the infiltrative process is strongly reduced.

In this case, only our data from Le Spesse spring were collected over a sufficiently long monitoring period. The monitoring period spanned from 1 October 2010 to 30 September 2011, during which time the discharge, temperature and EC data were monitored hourly.

The results show a correlation coefficient ( $\rho$ ) of -0.1. Thus, Le Spesse spring falls into type C (homogenization; Tab. 2).

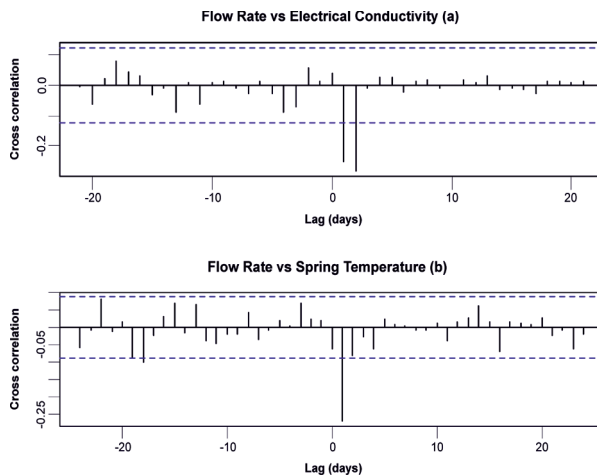


Fig. 16 - (a) CCF between spring flow rate and electrical conductivity; (b) CCF between spring flow rate and spring water temperature

Spring type and prevailing phenomena	Correlation coefficient ( $\rho$ )
Type A — Replacement	$-1 \leq \rho \leq -0.2$
Type B — Piston	$0.2 \leq \rho \leq 1$
Type C — Homogenization	$-0.2 \leq \rho \leq 0.2$

Tab. 2 - Spring categories (from GALLEANI *et alii*, 2011)

This result is in agreement with previous analyses, indicating that the initial increase of discharge was due to local infiltrating waters, and only after a period of time did the groundwater arrive from the deep reservoir.

A  $\beta$  factor of 2, a  $\gamma$  factor of 2.8 and a  $c(\rho)$  factor of 0.1 produce a VESPA index of 0.83, which places Le Spesse spring in the category of medium vulnerability ( $0.1 < V < 1$ ; Tab. 3).

Vulnerability	VESPA index
Very high	$V \geq 10$
High	$1 \leq V \leq 10$
Medium	$0.1 \leq V \leq 1$
Low	$0 \leq V \leq 0.1$

Tab. 3 - VESPA index (from GALLEANI *et alii*, 2011)

### ISOTOPIC ANALYSIS

In this study, an analysis of stable isotopes in waters, such as oxygen-18 ( $\delta^{18}O$ ) and deuterium ( $\delta D$ ), was also performed. Le Spesse and Ega Nass springs were sampled monthly from April to August 2011. Three rain samplers were installed, the first in Cava Buscada (municipality of Erto-Casso, at an altitude of approximately 1,750 m a.s.l.), the second in Le Spesse (in the same municipality, at an altitude of 810 m a.s.l.) and the third in Longarone (at approximately 450 m a.s.l.; Fig. 1). Beginning in April 2011, eleven samples of rainfall waters and sixteen samples of

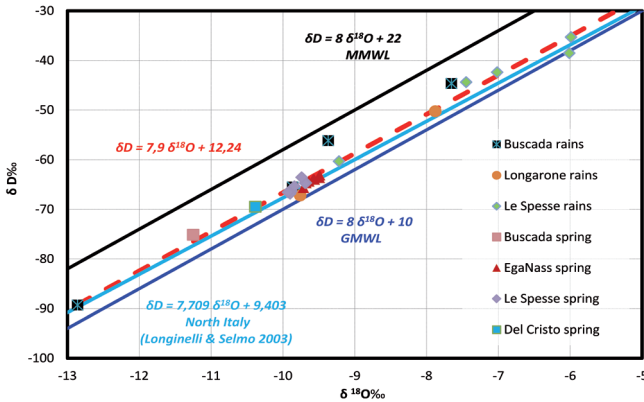


Fig. 17 - Isotopic diagram. Local Vajont line (dashed red line) in comparison with GMWL (solid blue line; CRAIG, 1961), MMWL (solid black line; GAT & CARMi, 1970) and North Italy (solid light blue line; LONGINELLI & SELMO, 2003)

spring water were collected. The samples were then analyzed at the Geosciences Department of Trieste University to measure their stable isotopic contents.

The derived (empirical) relationship between local  $\delta^{18}\text{O}$  and  $\delta\text{D}$  is as follows:

$$\delta\text{D} = 7.9 \delta^{18}\text{O} + 12.24$$

The highly correlative plot of the experimental data (coefficient of correlation of 0.98) and a high similarity between own experimental line and those from the literature (GAT & CARMi, 1970; CRAIG, 1961; LONGINELLI & SELMO, 2003; Fig. 17) indicate that evaporation in the Vajont area does not affect the amount of D and  $^{18}\text{O}$  in local rainfall and mixing with connate or very old waters may be excluded.

From Figure 17, it may be seen that the values of spring samples are less scattered/dispersed. An attenuation phenomenon of seasonal variations in spring waters is well known. As groundwater enters confined conditions, it is isolated from further seasonal and rainfall contribution and its isotopic compositions are attenuated to values representing a weighted mean of meteoric water inputs. The spring values show variation with respect to time, but while the variation in rainfall samples show a direct correlation with respect to air temperature, the spring samples show a shift in time. This phenomenon is observable both in the  $\delta^{18}\text{O}$  and  $\delta\text{D}$  contents (Fig. 18).

An explanation for this trend is that during summer the spring discharge mainly consists of water that infiltrated during the previous winter, as suggested by the comparison between discharge and water temperature. In fact, during the dry season the bulk discharge is from groundwater storage (fissure/porous matrix network; CLARK & FRITZ, 1997), whereas in the wet

season the groundwater is mixed with waters of local infiltration.

Even if few isotopic data are present, it is possible to assume that the phase shift of isotopic values in the spring water samples were due to the residence time of rainfall in the aquifer. This phenomenon is also known in the literature as *seasonal isotopic inversion* (LONGINELLI & SELMO, 2010).

Afterwards, the average value of rainfall isotopic composition was calculated to estimate a relationship between  $\delta^{18}\text{O}$  in local rainfall and elevation.

We were aware of the limited number of data and anomalous isotopic values found in the Longarone rainfall samples (elevation 450 m a.s.l.), which suggested that we eliminate these data from the estimation. Nevertheless, we estimated a theoretical meteoric local line of  $\delta^{18}\text{O}$  vs elevation (notwithstanding the evident limit of two available points). The  $\delta^{18}\text{O}$  and  $\delta\text{D}$  values found in the Longarone rainfall samples were more negative than those in Le Spesse rainfall samples (750 m a.s.l.). However, these anomalous values are common in the Alpine areas, and they are mainly related to the position of the mountains with respect to the direction of the prevailing wind and the prevailing trajectory of the rain-cloud front (LONGINELLI & SELMO, 2010).

When including only the Le Spesse and Cava Buscada  $\delta^{18}\text{O}$  average contents vs altitude, it was possible to estimate an approximate theoretical meteoric local line (Fig. 19), as follows:

$$\delta^{18}\text{O} = -0.0028 h - 5.0393$$

where h is the elevation (m a.s.l.).

The line shows an average gradient of -0.28‰ for every 100 m of elevation gain. This gradient is very similar to the medium line over the Adriatic slope presented by ZUPPI *et alii* (1974), as shown in Figure 19.

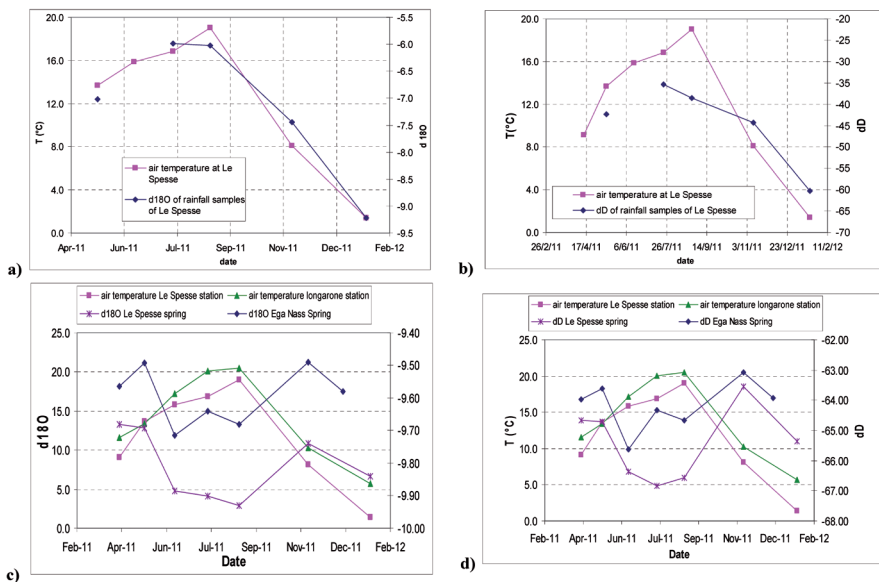
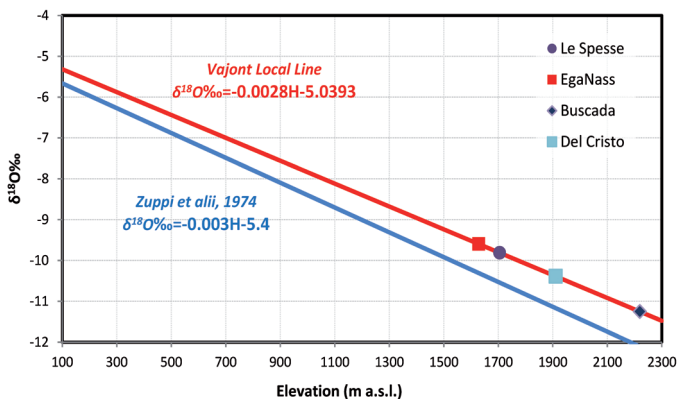


Fig. 18 - (a) Comparison between air temperature (T) and  $\delta^{18}O$  in rainfall at Le Spesse; (b) comparison between T and  $\delta D$  in rainfall at Le Spesse; (c) comparison between T at Le Spesse and Longarone and  $\delta^{18}O$  of Le Spesse and Ega Nass springs; d) comparison between T at Le Spesse and Longarone and  $\delta D$  of Le Spesse and Ega Nass springs

Fig. 19 - Diagram of  $\delta^{18}O$  versus altitude: medium local line in comparison with medium line of the Adriatic slope (ZUPPI et alii, 1974)



By calculating the average values of  $\delta^{18}O$  in spring water, it becomes possible, using the medium local line, to calculate the average elevation of water that recharges the aquifers supplying the springs in our study area. The calculated elevations of aquifer recharge water are approximately 1,700 m a.s.l. for Le Spesse spring, 1,600 m a.s.l. for Ega Nass spring, 2,200 m a.s.l. for Cava Buscada spring and 1,900 m a.s.l. for Del Cristo spring. The results show recharge rates that are in agreement with local hydrogeological and morphological conditions.

### HYDROGEOLOGICAL CONCEPTUAL MODEL

In a general conceptual model, the karstic reservoir may be thought of as two interconnected parallel flow systems, one associated with high-conductivity karstic channels and the other with a low-hydraulic-conductivity but high-storage-capacity, fissured, porous aquifer (BENISCHKE *et alii*, 1988; SEILER *et alii*, 1989; MALOSZEWSKI *et alii*, 2002). These two different parts of the aquifer hold different volumes of water. The first reservoir consists of a fissured, porous medium and contains a relatively large volume of water, whereas the second reservoir consists of karstic drain-

age channels containing little water.

In our springs, the conceptual model derives from analyses of diagrams displaying discharge, temperature and EC, different cross-correlations and the VESPA index, which are partially based on isotopic analytical results. In particular, Le Spesse spring shows a slow circulation of the deep reservoir water, and the high increases in discharge are essentially due to local infiltration rather than infiltration in the true (larger) recharge area (increases in discharge are associated with decreases in EC and T; there are positive cross-correlations between Ta and Ts). The comparison between discharge and temperature shows a decrease in Ts during the summer and an increase during the winter, indicating a discharge of deep reservoir water in partial thermal equilibrium with the rock matrix, and this seasonal trend was confirmed by the isotopic analytical results (seasonal isotopic inversion). A residence time of six months for the total spring flow is a relatively low value for karst aquifers.

The conceptual model is one of a regular discharge (base flow of deep waters) along with a local circulation directly linked to infiltration through the debris, which was confirmed by the correlation coefficient of

the VESPA index. The absence of a piston effect confirms the low level of karstification of this aquifer and a misleading karst response due to local infiltration.

The rainfall water enters the aquifer system at the surface of the catchment area and infiltrates down to karstic channels. From these channels, a portion of the water enters the fissure-porous aquifer. Water entering the karstic-fissured system from these channels contributes to the mean transit time of water in that system. The water in the channels finally discharges at the springs. The composition of the spring water is a weighted combination of water fluxes from both the karstic and fissured/porous sources. Thus, the karst is not well developed and its channels are of lesser hydrodynamical relevance than the fissured part of the reservoir.

## ACKNOWLEDGMENTS

This research was supported by a grant, *GEO-RISKS - Geological, morphological and hydrological processes: monitoring, modeling and impact in the north-eastern Italy*, funded by the University of Padova (Project Number STPD08RWBY\_001). The authors would like to thank an anonymous reviewer for helpful comments that contributed to improvements in the paper.

## REFERENCES

- AMIT H., LYAKHOVSKY V., KATZ A., STARINSKY A. & BURG A. (2002) - *Interpretation of spring recession curves*. Ground Water, **40**: 543-551.
- BELLONI L.G. & STEFANI R. (1987) - *The Vaiont slide: instrumentation-Past experience and the modern approach*. Engineering Geology, **24**: 445-474. doi: 10.1016/0013-7952(87)90079-2.
- BENISCHKE R., ZOJER H., FRITZ P., MALOSZEWSKI P. & STICHLER W. (1988) - *Environmental and artificial tracer studies in an Alpine karst massif (Austria)*. In YUAN D. & XIE C. (EDS.). *Karst hydrogeology and karst environment protection*. Proceedings IAH 21<sup>st</sup> Congress: Beijing, Geological Publishing House, 938-947.
- BESIO M. (1986) - *Hydrogeological notes regarding mount Toc and vicinity*. In: SEMENZA E. & MELIDORO G. (EDS.). Proceedings of the meeting on the 1963 Vaiont landslide. Convegno sulla frana del Vaiont, 133-155, Ferrara, Italy, 17-19- September-1986.
- CIVITA M. (1972) - *Schematizzazione idrogeologica delle sorgenti normali e delle relative opere di captazione*. Mem. e Note Ist. Geol. Appl., **12**, Napoli.
- CLARK I. & FRITZ P. (1997) - *Environmental isotopes in hydrogeology*. Lewis Publishers, CRC Press, Boca Raton - New York, 328 pp.
- CORBYN J.A. (1982) - *Failure of a partially submerged rock slope with particular references to the Vajont rock slide*. International Journal Engineering and Mining Sciences, **19**: 99-102. doi: 10.1016/0148-9062(82)91635-7.
- CRAIG, H. (1961) - *Isotopic variations in meteoric waters*. Science, **133**: 1702-1703.
- GALLEANI L., VIGNA B., BANZATO C. & LO RUSSO S. (2011) - *Validation of a vulnerability estimator for spring protection areas: the VESPA index*. Journal of Hydrology, **396**: 233-245.
- GAT J.R. & CARMÍ I. (1970) - *Evolution of the isotopic composition of atmospheric waters in the Mediterranean Sea area*. J. Geoph. Res., **75**: 3039-3048.
- GENEVOIS R. & GHIROTTI M. (2005) - *The 1963 Vaiont Landslide*. Giornale di Geologia Applicata, **1**: 41-53. doi: 10.1474/GGA.2005-01.0-05.0005.

- GHIROTTI M. (1994) - *Nuovi dati sulla frana del Vaiont e modellazione numerica*. Geologica Romana, **XXX**: 207-215.
- HELMSTETTER A., SORNETTE D., GRASSO J.R., ANDERSEN J. V., GLUZMAN S. & PISARENKO V. (2004) - *Slider block friction model for landslides: application to Vaiont and La Clapière landslides*. Journal of Geophysical Research, **109**: 1-15. doi: 10.1029/2002JB002160.
- HENDRON A.J. & PATTON F.D. (1985) - *The Vaiont slide, a geotechnical analysis based on new geological observations of the failure surface*. Tech Rep GL-85-5, 2 vols. Department of the Army, US Corps of Engineers, Washington, DC.
- HOBBS S.L. & SMART P.L. (1986) - *Characterization of carbonate aquifers: a conceptual base*. Proceedings 9<sup>th</sup> Congress of Speleology, **1**: 43-46.
- KILBURN C.R.J. & PETLEY D. N. (2003) - *Forecasting giant, catastrophic slope collapse: lessons from Vajont, Northern Italy*. Geomorphology, **54**: 21-32. doi: 10.1016/S0169-555X(03)00052-7.
- KRESIC N. & STEVANOVIC Z. (EDS.) (2009) - *Groundwater hydrology of springs*. Elsevier Inc., 565 pp. ISBN: 978-1-85617-502-9.
- LONGINELLI A. & SELMO E. (2003) - *Isotopic composition of precipitation in Italy: a first overall map*. Journal of Hydrology, **270**: 75-88.
- LONGINELLI A. & SELMO E. (2010) - *Isotope geochemistry and the water cycle: a short review with special emphasis on Italy*. Mem. Descr. Carta Geol. d'It., **XC**: 153-164.
- MALOSZEWSKI P., STICHLER W., ZUBER A. & RANK D. (2002) - *Identifying the flow systems in a karstic-fissured-porous aquifer, the Schnealpe, Austria, by modelling of environmental <sup>18</sup>O and <sup>3</sup>H isotopes*. Journal of Hydrology, **256** (1-2): 48-59.
- MEINZER O.F. (1923) - *The occurrence of groundwater in the United States*. Government Printing Office, USGS, Water Supply Paper 489. Washington D.C. (USA).
- MALVICINI C.F., TAMMO S.S., WALTER M.T., PARLANGE J. & WALTER M.F. (2005) - *Evaluation of spring flow in the uplands of Matalom, Leyte, Philippines*. Adv. Water Resour., **28**: 1083-1090. doi:10.1016/j.advwatres.2004.12.006.
- MANTOVANI F. & VITA-FINZI C. (2003) - *Neotectonics of the Vajont dam site*. Geomorphology, **54**: 33-37. doi: 10.1016/S0169-555X(03)00053-9.
- MÜLLER L. (1964) - *The rock slide in the Vajont Valley*. Rock Mechanics and Engineering Geology, **2**: 148-212.
- MÜLLER L. (1968) - *New considerations on the Vajont slide*. Rock Mechanics and Engineering Geology, **6**: 1-91.
- MÜLLER L. (1987) - *The Vaiont catastrophe: a personal review*. Engineering Geology, **24**: 513-523.
- NONVEILLER E. (1987) - *The Vajont reservoir slope failure*. Engineering Geology, **24**: 493-512, doi: 10.1016/0013-7952(87)90081-0.
- PLAGNES V. & BAKALOWICZ M. (2001) - *May it propose a unique interpretation for karstic spring chemographs?* In: Proceedings of the 7<sup>th</sup> Conference on Limestone Hydrology and Fissured Media, Besançon, France (20-22 September 2001), 293-298.
- SEMENZA E. & GHIROTTI M. (200) - *History of the 1963 Vaiont slide: the importance of geological factors*. Bull. Eng. Geol. Env., **59**: 87-97
- RIVA M., BESIO M., MASETTI D., ROCCATI F., SAPIGNI M. & SEMENZA E. (1990) - *La geologia delle valli Vaiont e Gallina (Dolomiti orientali)*. Ann. Univ. Ferrara Sez. Sci Terra, **2** (4): 55-76.
- SEILER K.P., MALOSZEWSKI P. & BEHRENS H. (1989) - *Hydrodynamic dispersion in karstified limestones and dolomites in the Upper Jurassic of the Franconian Alb, F.R.G.* Journal of Hydrology, **108**: 235-247.
- SEMENZA E. (1965) - *Sintesi sugli studi geologici sulla frana del Vajont dal 1959 al 1964*. Mem. Mus. Trentino Sci. Nat., **16**: 52 pp.
- TIKA T.H.E. & HUTCHINSON N. (1999) - *Ring shear tests on soil from the Vaiont landslide slip surface*. Geotechnique, **49**: 59-74.
- VEVEAKIS E., VARDOLAKIS I. & DI TORO G. (2007) - *Thermoporomechanics of creeping landslides: The 1963 Vaiont slide, northern Italy*. Journal of Geophysical Research, **112**: 1-21. doi: 10.1029/2006JF000702.
- VIGNA B. (2007) - *Classification and operation of aquifer systems in carbonate rocks*. Memorie dell'Istituto Italiano di Speleologia, **XIX**: 21-26. ISBN: 978-88-89897-03-4.
- WARD S.N. & DAY S. (2001) - *The 1963 Landslide and Flood at Vaiont Reservoir Italy. A tsunami ball simulation*. Ital. J. Geosci., **130** (1): 16-26.
- ZUPPI G.M., FONTES J.C. & LEOTOLLE R. (1974) - *Isotopes du milieu et circulations d'eaux sulfurees dans le Latium*. Proc. Symp. Isot. Techn. in Groundwater Hydrology, I.A.E.A., Vienna.

